UNDERSTANDING AND PREDICTING MICROBURSTS *

Marilyn M. Wolfson
MIT Lincoln Laboratory
Lexington, Massachusetts 02173

1. INTRODUCTION

Wind shear is a major cause of aircarrier accidents in the United States, and most of these accidents have been caused by one particular form of wind shear called a microburst (Zorpette, 1986). Microbursts have been defined as small scale, low-altitude, intense downdrafts which impact the surface and cause strong divergent outflows of wind. We know they are associated with thunderstorms and are usually but not always accompanied by heavy rainfall at the ground. However, a number of meteorologically distinct phenomena associated with thunderstorms can give rise to strong downdrafts and high surface winds. Most microburst research has focussed on the main precipitation driven downdraft of thunderstorms, both with and without significant surface rainfall. But other downdraft types such as the dynamically driven downdrafts at low altitude associated with "vortices" at the leading edge of expanding thunderstorm outflows and with "roll clouds" have also been associated with the microburst problem.

In this paper, I discuss these two primary forms of low altitude downdraft phenomena in thunderstorms. This differentiation is essential to discovering exactly what atmospheric conditions lead to the development of the most hazardous microbursts. A physically based predictive model for thunderstorm downdraft strength is presented which shows that the radar reflectivity of a storm alone cannot be used an a hazard index; information about the static stability of the atmosphere is also essential. I then show that the downdrafts associated with the gust front around a cold outflow from a small isolated thunderstorm, a microburst, are inherently stronger at low altitudes than those found in more straight-line gust fronts. Finally, I reexamine the most recent fatal U.S. microburst accident, the crash of Delta 191 at Dallas/Ft. Worth in 1985, and show that both types of low altitude downdrafts were encountered as part of the "microburst", although the downdrafts came from different storms.

2. THE MICROBURST AIRCRAFT HAZARD

Three major aircraft accidents account for all of the aviation fatalities attributed specifically to microbursts in the United States (see Table 1). The first of these – the crash of Eastern 66 at Kennedy airport in New York on 24 June 1975 (112 fatalities, 12 injuries) – led to the introduction by Fujita and Byers (1977) of the new downburst/microburst terminology. The two other fatal microburst accidents were Pan Am 759 at New Orleans International airport on 9 July 1982 (152 fatalities, 9 injuries), and Delta 191 at Dallas/Ft. Worth International airport on 2 August 1985 (130 fatalities, 31 injuries). No one escaped injury in any of these accidents. In all three of these cases, the thunderstorm downdraft implicated in the accident descended into a pre-existing outflow that was produced from a nearby thunderstorm. The presence of the turbulent gust front at the leading edge of the pre-existing outflow was not taken into consideration in assessments of the wind shear hazard in these cases.

In two of the four additional fatal accidents attributed to thunderstorm low altitude wind shear (Table 1), roll clouds were noted by eyewitnesses. These were the crash of a Braniff Airways plane at Falls City, NE on 6 August 1966 and the crash of an Ozark Air Lines plane St. Louis, MO on 23 July 1973. No one escaped injury in these two accidents, either. In the Falls City crash, "ground witnesses observed the aircraft to fly into or over a roll cloud preceding a thunderstorm and shortly thereafter saw an explosion in the sky followed by a fireball falling out of the cloud. Two pieces, later identified as major portions of the right wing and empennage, were seen falling separately from the main part of the aircraft. Shortly thereafter the witnesses noted high gusty surface winds and light to moderate rain which accompanied the passage of a squall line through the area. The cause of the accident was determined to be inflight structural failure caused by extreme turbulence" (Rudich 1986). Roll clouds mark the ascending branch of a horizontal vortex, usually either the gust front itself, a solitary wave, or part of an undular bore (Smith 1988). Before microbursts, gust fronts were considered the primary form of aviation hazardous low altitude wind shear. The information in Table 1 indicates that they are indeed extremely hazardous.

What role did the low altitude downdrafts and turbulence associated with the gust front at the leading edge of a pre-existing outflow play in the three microburst related fatal aircraft accidents? Certainly the divergent headwind–tailwind shear of the thunderstorm outflow itself can easily become strong enough to cause an unmanageable loss of lift to an aircraft penetrating it (Figure 1). Figure 2 shows that the magnitude of the downdraft velocity has as much effect as the horizontal wind shear on the ability of a plane to maintain its speed and glide slope profile. But Figure 2 also shows that even performance increasing wind shear (increasing headwind) and updrafts, typically associated with gust fronts, can be unsafe when their magnitudes are large. The effect of *turbulence* on aircraft control is not captured by the F-factor index, but the hazard can be extreme, especially at low altitudes.

I suggest that the pre-existing gust front in each of the fatal microburst accident cases may have added a crucial ingredient to the overall hazard encountered. When a thunderstorm outflow forms on top of an existing gust front, two hazardous regions become juxtaposed that would otherwise be physically separate. This *combination* may be what was first called a downburst, and later a microburst, by Fujita and Byers (1977).

*The work described here was sponsored by the Federal Aviation Administration. The United States Government assumes no liability for its content or use thereof.

Table 1 . Aircraft accidents in the United States attributable to microbursts or low altitude wind shear associated with thunderstorms. Wind speed is given in meters per second, and cell diameters are given in kilometers. F/I/U indicates number of fatalities, injured, and uninjured. Information adapted from Viemeister (1961), Fujita (1985), Rudich (1986), and Laynor (1986). MB *indicates microburst.*

Location	Date	Winds	Diameter	Rain	Weather	F / I / U
Bowling Green	28 Jul 43	strong	10–15	yes	strong squall wind from violent downdraft fanning out at surface; unusually severe turbulence	?/ ?/ 2
Mason City, IA	22 Aug 54	35–40	5	heavy	plane entered thunderstorm at 400–500 ft; sank in downdraft	12/ 7/ 0
Rochester NY	2 Jul 63	shifting	?	heavy	thunderstorm approaching runway from west, plane took off into heavy rain and shifting winds	7/ ?/ ?
Falls City, NE	6 Aug 66	gusty	n/a	light	roll cloud preceding thunderstorm; severe turbulence	42/ 0/ 0
St. Louis	23 Jul 73	strong	?	heavy	severe thunderstorm with roll clouds, heavy rain, strong winds	38/ 6/ 0
Chattanooga	27 Nov 73	?	?	heavy	low altitude wind shear existed in heavy rain on approach	0/42/37
New York	24 Jun 75	10–17	5–10	heavy	hot smoggy day, seabreeze; light, moderate, & heavy rain; numerous small cells, spearhead echo 8 x 32 km; MB	112/12/ 0
Denver	7 Aug 75	>12	2	light	numerous scattered showers–small and weak; cell broke into two, thunder heard, spearhead echo 8 x 16 km; MB	0/15/119
Raleigh–Durham	12 Nov 75	?	?	heavy	unexpected heavy rain, windshear and downdraft at 100 ft agl	0/ 1/138
Philadelphia	23 Jun 76	20	4	yes	headwind increase in front of shower; scattered showers and thunderstorms near warm front, growing spearhead echo 13 x 27 km; MB	0/86/20
Tucson	3 Jun 77	14	2	none	numerous CB around airport; gust front passed with 25 m/s surface winds; MB	0/ 0/ALL
New Orleans	9 Jul 82	>15	2	heavy	scattered showers, 7 gust fronts nearby, recent growth of convective cloud tops; MB	152/ 9/ 0
Detroit	13 Jun 84	10–16	?	heavy + hail	thunderstorm with heavy rain; 3/4 inch hail at 100–200 ft agl; turbulence, severe wind shear	0/ 0/ALL
Dallas	2 Aug 85	22–35	4	very heavy	scattered small cells initiated on gust front out of large cell to NW, very hot day, cloud top of MB cell 23 Kft (questionable – NTSB reported 40–50 Kft.); MB	130/31/ 0

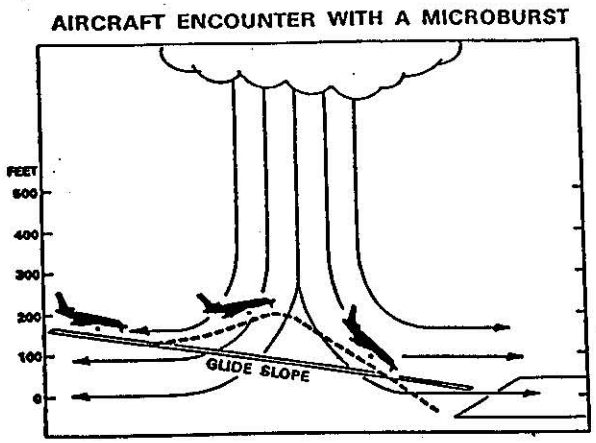

Figure 1 . Schematic drawing of an aircraft encounter with a microburst. Notice that the increased headwind lifts the plane above its intended glideslope while the increased tailwind causes the plane to fall below its intended glideslope. This simplified view of a microburst is inaccurate because it does not depict the extremely turbulent vortex at the leading edge of the outflow.

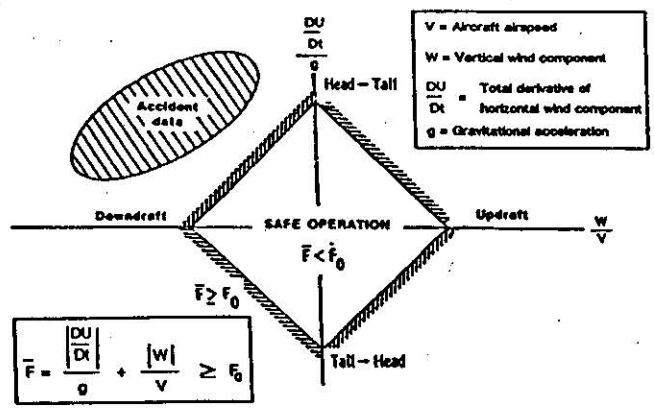

Figure 2 . Definition of F-factor wind shear hazard index. Typical threshold values (F_0) for jet transport range from 0.10 – 0.15. Notice that all of the aircraft accidents are thought to have taken place in the quadrant associated with divergent horizontal winds and downward vertical velocities along the flight path. Adapted from Targ and Bowles (1988).

3. PREDICTING THUNDERSTORM DOWNDRAFT AND OUTFLOW STRENGTH

Certainly a newly formed thunderstorm downdraft and surface outflow were key factors in all the microburst aircraft accidents. In this section, I focus on the identification of observable parameters that will allow quantitative prediction of the eventual maximum downdraft and outflow strengths.

A great deal of research over the last few years has attempted to quantify the factors influencing the development of the strongest thunderstorm downdrafts and outflows. One of the apparent mysteries is that thunderstorms with quite different downdraft and outflow strengths can occur simultaneously, in the same environment. Even when the reflectivity or water content of these cells is taken into account, differences remain that are related to cell forcing, geometry, or the proximity and strength of neighboring convection. Another apparent mystery is that storms with similar reflectivity levels on different days produce very different strength outflows. Because of the proportionality between reflectivity and the downward acceleration due to water loading, some argue there should be a monotonic relationship between downdraft/outflow strength and reflectivity. Yet evidence is to the contrary (e.g., Wilson et al. 1984; Biron and Isaminger 1989). This is, in part, because environmental factors that promote the thermodynamic generation of negative buoyancy are of crucial importance in determining the ultimate downward acceleration and observed downdraft strength. Subtle differences in the vertical temperature structure of the environment, such as the existence and height of any elevated stable layers or inversions, also play an important role in determining the ultimate downdraft strength (Knupp 1987).

3.1. Model Derivation

Although a number of observational studies on determining reliable precursors for microbursts have been performed (e.g., Campbell and Isaminger 1989; Potts 1989), none have gone beyond basic statistical correlation of these precursors with resultant outflow strength. The approach used here is to quantitatively predict thunderstorm downdraft and outflow strength with a simple model based on the vertical momentum and continuity equations. The published axisymmetric numerical thunderstorm model output of Proctor (1989; referred to as P89), Krueger and Wakimoto (1985; KW) and Droegemeier and Babcock (1989; DB) is used as "data" to derive the model. Details of the derivation not presented here can be found in Wolfson (1990).

The vertical momentum equation is used to indicate the expected dependence of the vertical velocity on the various forcing mechanisms at work in the thunderstorm downdraft. Neglecting entrainment, the Boussinesq form of the vertical momentum equation can be written as:

$$\frac{dw}{dt} = g\frac{\theta'}{\theta_0} - g\,(l+i) - \frac{P'_z}{\rho_0} \qquad (3.1)$$

where w is the vertical velocity, t is time, g is the gravitational acceleration, θ_0 is the potential temperature of the environment which varies only in height and θ' is the difference in potential temperature between a parcel and the environment, $(l+i)$ is the mass mixing ratio of liquid water plus ice, P' is the perturbation pressure, ρ_0 is the density which varies only in height, and the subscript z denotes partial differentiation in height. Perturbation pressure buoyancy itself (as opposed to its vertical gradient) and frictional effects are ignored. Buoyancy effects of humidity in the environment have not been included but they can be easily by substituting virtual potential temperature for θ in Eq. (3.1).

The rationale behind the model development is to relate each term in the vertical momentum equation to the observable environmental or storm characteristics that are physically responsible for its ultimate magnitude. A number of simplifying assumptions have to be made. The total vertical acceleration is approximated as:

$$\frac{dw}{dt} \sim \left(\frac{w^2}{2}\right)_z \qquad (3.2)$$

This represents the left hand side of Eq. (3.1). Making this substitution, and integrating Eq. (3.1) in height, the following dependence of the vertical velocity on the depth of the downdraft column results:

$$w^2 \sim forcing \cdot \Delta z$$

Knupp (1987) showed that this downdraft depth can be related to the "transition level" in the sounding. The downdraft velocity data from the cases he investigated do show this square root dependence on the height of the transition level. Addis (1984) showed a similar dependence of the vertical velocity on the height of the downdraft column in his convective storm outflow modelling work.

The first term on the right hand side of Eq. (3.1) is the temperature buoyancy. For a given condensate mixing ratio, the downdraft velocity will increase as the lapse rate in the subcloud environment increases from stable toward neutral values, largely because of the resultant temperature buoyancy contribution to the vertical acceleration. Studies have shown that for strong downdrafts and outflows to occur at lapse rates below about 7 K/km, high reflectivity must be present. However, when the lapse rate approaches the dry adiabatic value, almost any concentration of precipitation can produce strong downdrafts, especially if the subcloud layer is deep. Srivastava (1985) calculated the temperature excess of descending air parcels over their ambient environment for various subcloud lapse rates and liquid water mixing ratios, using a model based on evolution equations for raindrop mass and size distribution, thermodynamic energy, water substance, and vertical velocity. His tabulated data show a quadratic dependence of this temperature difference on lapse rate for a given liquid water mixing ratio:

$$\theta' \sim \Gamma^2 \quad \text{or} \quad w^2 \sim \Gamma^2\,\Delta z \qquad (3.3)$$

where G is the temperature lapse rate. By comparison with the axisymmetric numerical model data of KW(Figure 3), it was discovered that this relationship does indeed hold true for a given precipitation mixing ratio. As the mixing ratio increases, greater downdraft velocities are achieved, but the linear dependence of vertical velocity on lapse rate does not vary much. The mixing ratio dependence of the temperature buoyancy represents one part of the vertical acceleration due

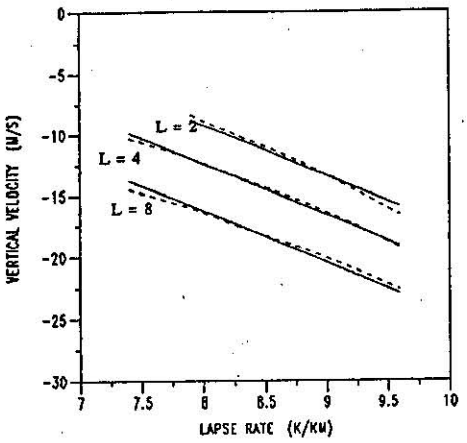

Figure 3 . Plot of the vertical velocity (w) vs the environmental lapse rate (Γ) from the numerical simulations by Krueger and Wakimoto (1985), for liquid water mixing ratios (L) of 2, 4, and 8 g/Kg (dashed lines). The solid lines represent the best fit for each mixing ratio using the mean of the slopes derived from the least squares linear fit for each mixing ratio curve individually: $w_2 = -4.175\ \Gamma + 24.19$; $w_4 = -4.175\ \Gamma + 20.99$; $w_8 = -4.175\ \Gamma + 17.14$.

to total water concentration, and can be represented by an undetermined function of the mixing ratio:

$$w^2 \sim [\ \Gamma^2 + f(L)\ ]\ \Delta z \ .$$

Note that L is used to represent the total mixing ratio instead of $(\ l + i\ )$ as in Eq. (3.1) because no account is taken of the phase of the water mass present. The temperature buoyancy effects from the total water content can be quantitatively incorporated in the precipitation loading term.

The second term on the right hand side of Eq. (3.1) is the contribution of precipitation loading to the vertical acceleration. The form of that term, combined with the simplifying approximation of Eq. (3.2), gives the following dependence of the vertical velocity on the precipitation content:

$$w^2 \sim L\ \Delta z \ .$$

Comparison with numerical model results of KW and DB showed that if L was interpreted as the peak value of a Gaussian distributed precipitation region, then the vertical velocity also depended equally strongly on the vertical depth (Gaussian half amplitude width in the vertical) of that precipitation region. Representing this depth as D, the velocity dependence can be expressed as:

$$w^2 \sim L\ D\ \Delta z \ .$$

The parameters L and D will ultimately be estimated from radar reflectivity which depends strongly on the precipitation drop size distribution present in the storm. Many equations relating reflectivity to water content that account for these different distributions have been derived. The choice of equation will depend on the type of convection present (perhaps the peak reflectivity observed), the climatic region, the season of the year, etc. All of the known dependence of the vertical velocity on precipitation size distribution and phase will be contained in this choice.

The third and final term on the right hand side of Eq. (3.1) is proportional to the vertical gradient of the perturbation pressure. For this thunderstorm downdraft application, the pressure perturbation of interest is created largely by the descending downdraft itself, and it generally opposes the downward motion. If all other forcing remains equal, the downdraft velocity will vary inversely with the downdraft radius at large radii, because of the induced pressure perturbation (P89, KW). But the same induced pressure perturbation sets up the horizontal pressure gradient that ultimately drives the divergent surface outflow as the downdraft reaches the ground; the pressure is thus the connection between the downdraft and outflow. Based on the continuity of mass and on dimensional grounds, it can be seen that:

$$\frac{u}{w} \sim \frac{width}{height} \sim \frac{1}{A}$$

where u is the outflow velocity from a cylindrical downdraft reaching the ground, and A is the aspect ratio of the downdraft defined as the ratio of its height to width. The third term on the right hand side of Eq. (3.1) will be neglected, and the pressure effects will be incorporated in a prediction equation for the ratio u/w.

The predicted outflow speed will depend not only on the vertical velocity and the aspect ratio of the downdraft, but on the temperature of the downdraft (outflow) air as well. Fawbush and Miller (1954) modelled this dependence of horizontal wind speed with a cubic equation in temperature based on observations, but P89 recently found that a linear relationship was roughly as accurate. However, there are no theoretically obvious reasons for either the cubic or linear relationships. One theoretical guideline that could be used is the well known equation for the speed of the leading edge of a density current that is thin relative to the depth of the fluid in which it is propagating (e.g., Simpson 1987):

$$V = \sqrt{2\ g\ h\ \frac{\Delta\rho}{\rho}}$$

where V is the gravity current speed, $\Delta\rho$ is the density difference across the front, ρ is the density of the less dense fluid, and h is the depth of the density current. The horizontal flow behind the leading edge is often faster than, but directly proportional to the speed of the front, so the dependence on density difference should be the same. Since the magnitude of the fractional potential temperature difference across the front is proportional to that of the fractional density difference, Eq. (3.3) would imply the outflow speed was related linearly to the lapse rate:

$$\frac{u}{w} \sim \Gamma \ .$$

Comparison with numerical modelling results showed there was indeed a dependence of the outflow speed on the lapse rate that could be modelled as linear, but not enough data were available to determine if the dependence was of higher order or not. Thus a linear dependence between the outflow speed and the lapse rate was assumed, and the best fit coefficients were derived.

3.2. Prediction Equations

In the preceding section, the dependence of vertical velocity on the radius and depth of the precipitation core, the precipitation mixing ratio, the environmental temperature lapse rate, and the height of the transition level was inferred by simple physical arguments. These results were confirmed through comparison with results from the published axisymmetric numerical modelling studies of P89, KW, and DB. These quantitative results were combined to yield:

$$W^2 = [\,7.3\,\Gamma^2 + 9.75\,L\,D - 480\,]\,\frac{T_r}{3.3} \qquad (3.4)$$

where W is the maximum downdraft velocity in m/s, Γ is the mean temperature lapse rate from the surface to the freezing level in K/km, L is the precipitation mixing ratio in g/Kg, D is the depth of the precipitation core in km, and Tr is the transition level of the sounding in km. If evaluating the terms on the right hand side of Eq. (3.4) produces a negative number, W should be interpreted as negligibly small.

The dependence of the ratio of the maximum outflow speeds (U) to the maximum downdraft speeds (W) was found to depend strongly only on the aspect ratio (A) of the precipitation core (i.e. ratio of vertical to horizontal extent), with a weak dependence on the environmental lapse rate. These results were combined into a predictive equation for the ratio U/W which, when combined with Eq. (3.4), provides a predictive equation for U alone:

$$\frac{U}{W} = \left(\frac{.75}{A} + .65\right)\frac{\Gamma}{9} \qquad (3.5)$$

where all of the variables have been defined above. If the predicted value of U/W is less than 1.0, the value should be set equal to 1.0. For example, when the lapse rate is dry adiabatic, $U/W = 1$ for aspect ratios ≥ 2.75.

In applying Eqs. (3.4) and (3.5), a three dimensional radar reflectivity field would be searched for storm "cells", significant maxima in the field, to locate the sites of potential strong downdrafts. A bi-Gaussian distribution would then be fit to these regions, after they had been converted from reflectivity to water mixing ratio. The peak value of the Gaussian mixing ratio distribution would be used for L, the depth at half maximum for D, and the ratio of D to the width at half maximum would be used for A. Because information on the downdraft width is available through application of this model, the surface divergence as well as the downdraft and outflow speeds can be predicted. Indicators of aircraft performance loss that depend not only on the differential velocity, but on the horizontal divergence and the vertical velocity as well, can readily be calculated (e.g., F-factor index, Frost and Bowles 1984; see Figure 2).

3.3. Application of Model

Recent papers by Wakimoto and Bringi (1988) and Kingsmill et al. (1989) gave enough data on a "strong" airmass thunderstorm that occurred near Huntsville, AL on July 20, 1986 to estimate the parameters needed for predicting the downdraft and outflow velocities via Eqs. (3.4) and (3.5), and to compare the predictions with what was actually observed. Enough data were also presented for predictions on two other storms, July 13 and July 16, 1986. Wakimoto and Bringi (1988) noted that the soundings on these two days were similar to the July 20 sounding, but that these storms resulted in only "weak" and "moderate" outflows, respectively.

To estimate the parameters needed for the prediction equations, the reflectivity values were first converted to liquid water content using an equation derived by Burrows and Osborne (1986) for the volume concentration of water, and normalized by the ambient density. A Gaussian shape was subjectively fitted to the resulting distribution to give the liquid water content at the peak (L), the core depth (D; the Gaussian width at half amplitude), and the core aspect ratio (A). By fitting a bi-Gaussian distribution to the liquid water content field, the data characteristics match as closely as possible the water content fields used to initiate the numerical models from which the equations were derived. The other required parameters were derived from the published soundings.

The model estimates for these three high reflectivity cases are compared with the actual data in Table 2 . The simple model given by Eqs. (3.4) and (3.5) has correctly ranked these quite different storms occurring in similar environments, according to their outflow strength. This suggests that thunderstorm downdraft and outflow strength might be predicted quite adequately with standard radar reflectivity data and a proximity sounding. Because radar reflectivity increases when frozen condensate melts, part of the increased acceleration from the thermodynamic effects of ice is incorporated even in this simple model.

Wakimoto et al. (1989) studied a low reflectivity storm that occurred in the Denver area on July 9, 1987 with multiple Doppler radars and photogrammetric analyses. The model estimates for this case are also given in Table 2 . In

Table 2 . Application of predictive model to 4 storm cases. The variables given are identified in Eqs. (3.4) and (3.5). The asterisks indicate outflow values estimated from single Doppler radar data; the vertical velocities for those cases were not estimated. The other data were derived from multiple Doppler analyses.

Jul 20 '86	A	D	dBZ	L	Tr	Γ	W	U
(Strong)	1.8	2	63	27	2.2	7.2	16.8	16.8
						actual:	13	17
Jul 13 '86	**A**	**D**	**dBZ**	**L**	**Tr**	**Γ**	**W**	**U**
(Weak)	1.25	1.5	57	10	2	7.0	4	4
						actual:	?	7 *
Jul 16 '86	**A**	**D**	**dBZ**	**L**	**Tr**	**Γ**	**W**	**U**
(Moderate)	1.0	2	60	34	1.2	7.0	14	14
						actual:	?	9 *
Jul 9 '87	**A**	**D**	**dBZ**	**L**	**Tr**	**Γ**	**W**	**U**
(Low dBZ)	1.0	2	25	0.2	4	9.4	14.3	21.5
						actual:	13.4	> 15

contrast to the previous high reflectivity cases, this case had only 25 dBZ or 0.2 g/Kg peak water content in the core. Thus the second term on the right hand side of Eq. (3.4) is essentially negligible in this case. Again in contrast to the first three cases, the first term on the right hand side of Eq. (3.4) is very large in this case because of the nearly dry adiabatic lapse rate between the surface and the freezing level. The result is a downdraft and outflow strength comparable to the "strong" high reflectivity storm of July 20, 1986.

3.4. Summary

The ability of the model given by Eqs. (3.4) and (3.5) to correctly rank, and fairly closely estimate, the eventual downdraft and outflow velocities in these four quite different cases adds confidence to the assertion that it approximately captures the essential physics of accelerating downdrafts and outflows. By developing a physically based predictive system, there is hope that the system can remain reliable as the storms it has to detect change from the very dry virga shafts typical of the Denver area to the very wet thunderstorms in the humid southeastern part of the country. This model shows that the radar reflectivity of a storm alone cannot be used as a hazard index; information about the static stability of the lower atmosphere is also essential.

4. LEADING VORTEX RING IN AXISYMMETRIC OUTFLOWS

The most important low altitude downdrafts in thunderstorm outflows, apart from the central precipitation driven downdraft, are those associated with the "vortex" that develops at the leading edge of the dense outflow, the gust front. As mentioned previously, in all three of the fatal microburst aircraft accidents, a gust front from an older thunderstorm outflow was present when the thunderstorm outflow implicated in the accident occurred.

While every gust front has a horizontal vortex circulation associated with the "head" (Figure 4), the circulation

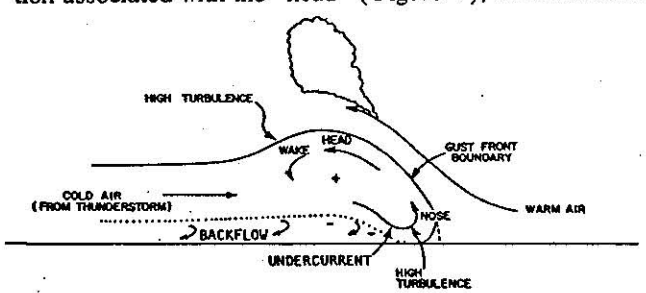

Figure 4 . Schematic representation of an atmospheric density current. Taken from Goff (1976).

is much more pronounced relative to the depth of the outflow in an axisymmetric outflow than in a unidirectional flow. Strong surface winds and strong downdrafts *at low altitudes* will be associated with this leading vortex region, as will extreme turbulence. It is thus a very important part of the microburst problem, and needs to be understood. In this section, I focus on explaining the leading vortex ring structure of gust fronts from axisymmetric outflows.

4.1. Observations

Figure 5 shows the surface reflectivity of a strong, isolated microburst observed with the FAA-Lincoln Laboratory Terminal Doppler Weather Radar (TDWR) testbed (Evans and Turnbull 1989) near the Memphis International airport on 26 June 1985. Observers noted extremely heavy precipitation during this storm. Taking as time T the time shown in Figure 5 (a), the evolution of the outflow at five times from T+1.5 min to T+5.6 min is shown in Figure 5 (b). The high reflectivity (45–55 dBZ) main storm

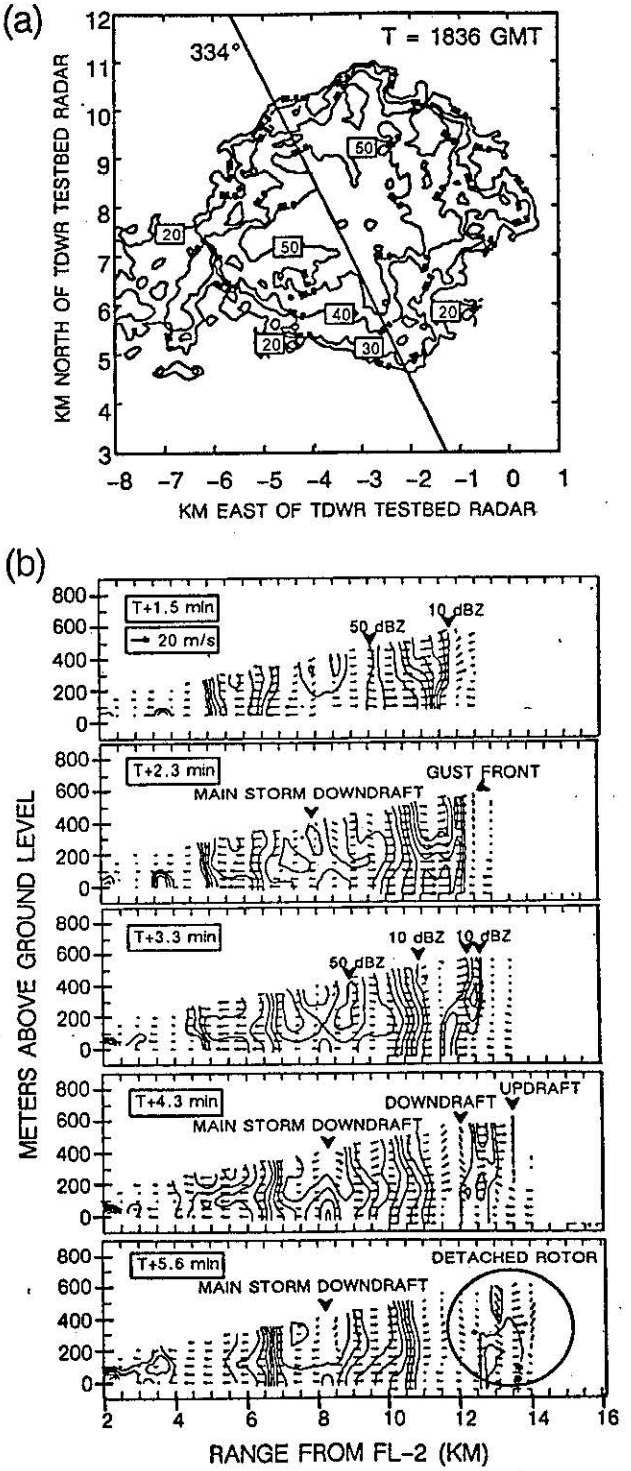

Figure 5 . (a) TDWR testbed radar 0.5° elevation scan at time T, 1836:29 GMT, on 26 June 1985. Data were collected near Memphis, TN. Reflectivity is contoured at 20, 30, 40, and 50 dBZ (selected contours are labelled with boxed numerals). (b) Vertical cross-sections along azimuth 334° [shown in (a)], at five sequential times. Reflectivity is contoured every 5 dBZ from 10 dBZ.

downdraft is located at a range of approximately 8 km from the TDWR testbed radar in these cross-sections. The strongest outflow winds are located approximately 100 m agl. The cross-sections clearly show the development of a horizontal vortex or "rotor" associated with the leading gust front as the outflow spreads away from the storm center. This vortex eventually detaches and moves away from the main outflow.

4.2. Physical Explanation of Leading Ring Formation

This process of formation of an intense leading "vortex ring" in an axisymmetric gravitational flow has been qualitatively explained as a result of radial expansion of the circumference, and thus the head wave vortex axis, of the dense outflow (Fujita 1984; see Figure 6). The argument

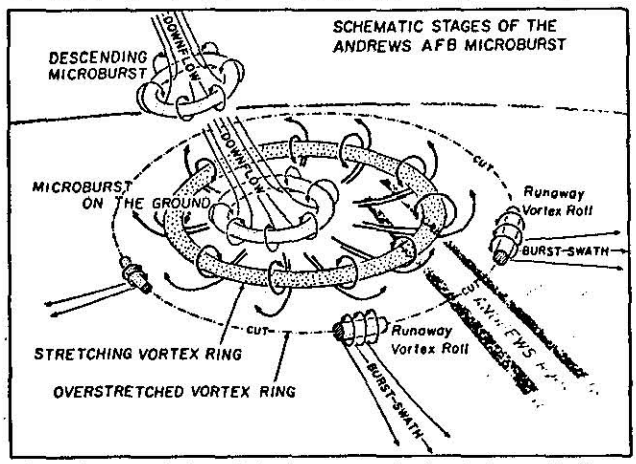

Figure 6 . Depiction of the four stages in the Andrews Air Force Base microburst by Fujita (1984).

offered is that, "because the fluid volume in a vortex is (approximately) conserved, its cross-sectional area must decrease. Conservation of angular momentum about the center line of the vortex then implies that the vorticity increases." (Linden and Simpson 1985). This qualitative model for the leading vortex in dense axisymmetric outflows has been inconsistently formulated without the benefit of complete observations. It is essentially incorrect; the volume of the leading vortex is not conserved but steadily increases with time.

The correct model for understanding the formation of a leading vortex ring in dense, axisymmetric outflows has been described by Garvine (1984). Garvine modelled the case of a radially spreading surface buoyant flow with a continuous source to help explain the observed characteristics of river plumes, created where fresh water empties into coastal seawater. A thin layer of buoyant water spreads radially under the force of gravity, with a sharp frontal boundary at the leading edge.

The main body of the plume is modelled using the inviscid nonlinear shallow water equations, and the frontal boundary is represented by a jump condition. The Boussinesq approximation is made, and wind stress, mixing, and the Coriolis acceleration are all neglected. The difference in density between the buoyant fluid and the surrounding fluid is constant, so the radial pressure gradient and the fluid velocity are vertically uniform. With these approximations, the governing equations of mass continuity and radial momentum for the main plume body are:

$$(c^2)_t + \frac{(rc^2u)_r}{r} = 0$$

$$u_t + \left(\frac{u^2}{2} + c^2\right)_r = 0$$

where $c \equiv \sqrt{(g'd)}$ is the long internal wave speed (g' is the reduced gravity, and d is the depth of the gravity current), t is the time from initial fluid release, r is the radial distance from the source center, u is the radial velocity, and the subscripts denote partial differentiation with respect to that variable. These two equations together form a hyperbolic system with a pair of characteristic lines given locally by:

$$\frac{dr}{dt} = u \pm c \qquad (4.1)$$

along which the corresponding characteristic equations are:

$$du \pm 2\,dc = \mp \frac{cu}{r}\,dt \qquad (4.2)$$

The "+" (upper) and "–" (lower) families of characteristics represent the nonlinear, internal gravity waves that propagate upstream and downstream, respectively, at phase speed c relative to the outflow, and at absolute wave speed $u \pm c$ relative to fixed coordinates. The equations corresponding to Eqs. (4.1) and (4.2) for parallel flow are identical except for the term on the right hand side of (4.2), which represents the effects of radial expansion on the flow.

The results of a sample calculation with no entrainment are shown in Figure 7 . The scaled interface depth of

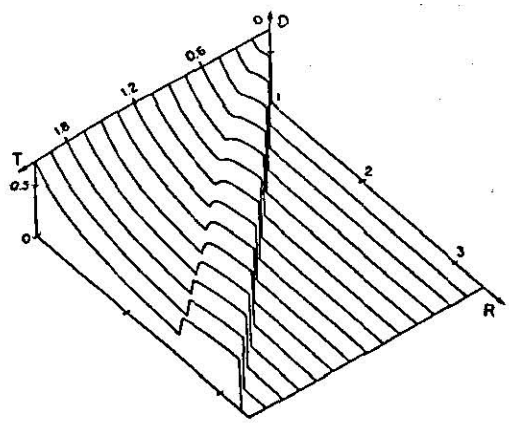

Figure 7 Isometric projection of scaled interface depth (D) as a function of scaled range (R) and time (T). Taken from Garvine (1984).

the modelled river plume is shown, but this can also be interpreted as the interface height of a cold thunderstorm outflow. The most prominent feature of the flow is the clear emergence of a ridge, at first indistinct, but later quite distinct with a sharp dip (dubbed the "trailing front", in contrast to the "leading front"). This trailing front became so steep that Garvine treated it numerically as a second front with its own jump conditions. The width of the ridge or ring feature increases with time, and the interface height within the ring is about 20% greater at the leading front than at the trailing front.

As the fluid expands radially, the fluid at the leading edge of the current begins to accelerate outward. However, the acceleration of the fluid just behind the front is limited by the front itself, and these disturbances will propagate back away from the front. The first waves to be reflected off the leading front (minus family) have low initial wave speed ($u - c$), since c is relatively high in the deeper flow near the front. They are later overtaken by reflected waves from further upstream in the ring, nearer the steady spreading regime. This overtaking is in the form of wave coalescence, a necessary condition for the formation of an interior front. The reflected waves continue to accumulate within the ring at the trailing front, causing the trailing edge of the ring to deepen.

The volume of the ring feature, proportional to the product of the mean radius and the ring width and depth, continually increases with time as a result of inflow into the ring through the trailing front. In the case of no entrainment, it had increased by a factor of 6 by the time the leading front had reached a distance of about 10 times the source radius. With entrainment, the results are qualitatively the same, but the increase in volume is not as marked because fluid in lost at both fronts. This basically refutes the argument that the frontal ring in axisymmetric outflows is a vortex tube that undergoes stretching as the flow expands.

In a parallel, two dimensional flow released from a line source, both plus and minus families of characteristics would be straight lines, corresponding to internal waves of *zero* amplitude. All properties of the flow except for the position of the front would be uniform in time and space. No changes in the flow state would occur, and to an observer moving with the flow at the frontal speed, the flow would appear steady. Neither the trailing front nor the radial ring would form.

4.3. Summary

The gust front at the leading edge of the cold outflow from a small, axisymmetric thunderstorm (e.g., Figure 5) is fundamentally different from its more straight line counterpart, either from a very large circular storm or a line storm (e.g., Figure 4). The rapid build up of fluid at the gust front edge only occurs in small, axisymmetric outflows where the radial expansion of the flow is large. This fluid in the leading "vortex" ring is extremely turbulent, and contains violent updrafts and downdrafts; it represents a very significant part of the microburst hazard. Moreover, the fluid ring is quite stable and can persist long after the primary divergent outflow has dissipated. The idealized outflow from a small isolated cell with no leading vortex front (Figure 1) essentially never occurs.

5. FATAL MICROBURST AIRCRAFT ACCIDENTS

In the preceding two sections, I have discussed the important hazardous low altitude downdrafts in thunderstorm outflows: 1) the precipitation driven downdraft, coincident with the reflectivity core, and 2) the downdrafts associated with the gust front at the leading edge of the outflow. I suggest that both of these types of downdrafts were involved in each of the fatal U.S. microburst aircraft accidents: JFK 1975, New Orleans 1982, and DFW 1985.

The most recent of these accidents was the crash of Delta Flight 191 at Dallas/Ft. Worth airport on August 2, 1985. There was a digital flight data recorder on board the aircraft, so it was possible to recover unambiguously the three dimensional wind field through which the aircraft flew (Wingrove and Bach 1987). I will focus attention on the DFW accident since the data are far less ambiguous than those available from the other two accidents.

5.1. Hypothesized Scenarios for DFW Accident

Several conceptual models and hypotheses have been offered to explain the meteorological events giving rise to the measured winds, especially the short wavelength "vortices" or rapid oscillations in wind components and temperature encountered during the last 20 s of the flight. These conceptual models all include a recently developed thunderstorm outflow with a radius of 2 km, at the following locations relative to the north end of runway 17L:

0.15 km west	3.5 km north	Fujita (1986)
0.5 km west	3.6 km north	Caracena et al. (1986)
0.6 km east	3.5 km north	Proctor (1988)

Hypotheses for the vortices include:

Fujita (1986): Three concentric downdraft outflows; Caracena (1987): Old vortices formed around downdraft and injected into outflow; Linden and Simpson (1986) and Droegemeier and Babcock (1989): Finite amplitude Kelvin–Helmholtz billows; Wolfson (1990): Cylindrical solitary waves.

These hypotheses are all quite plausible mechanisms for creating vortices under some circumstances. The question is, can they really account for the observed wind shear pattern encountered by Delta 191 at DFW? One way to test these hypotheses is to try to simulate the suggested scenario with numerical models.

With the help of Drs. John Anderson and Jerry Straka at the University of Wisconsin, an axisymmetric numerical experiment was performed with Anderson's (1990) model to test Fujita's "three concentric downdrafts" hypothesis for the DFW vortices. We modelled this as a single pulsating cylindrical downdraft. The horizontal and vertical grid resolution was 75 m, the time step 0.5 s, the domain 300 grid points wide by 100 high, and the eddy diffusion coefficient 40 m^2/s. The environmental lapse rate was dry adiabatic (300 K) up to 5 km agl, and stable above (4 K/km). The cooling source was Gaussian in shape, with a radius of 1.5 km, and a depth of 4 km, centered 3.75 km above the surface. The cooling function for each experiment is shown in Figure 8 (a). A 6 min pulsing frequency was chosen because it was the shortest period for which distinct features remained resolvable in the outflow and because rainfall data frequently show surges with approximately this time scale.

The first two cycles of the pulsing experiment (12 min) essentially created the surface outflow. The cold air pulse created by the cooling cycle that peaked at 13.5 min can be followed as it falls into the pre–existing outflow and moves toward the front [Figure 8 (b)]. By 20 min, a distinct subfrontal feature has formed, and it is clear from the time evolution that it propagates relative to the surrounding current toward the front. By 22 min into the simulation, another sharpening pulse of cold air from the cooling maximum at 19.5 min can be seen beginning to move out into the current. Each pulse has a horizontal circulation associated with it that is less intense than, but in the same sense as the circulation associated with the gravity current front. By 26 min,

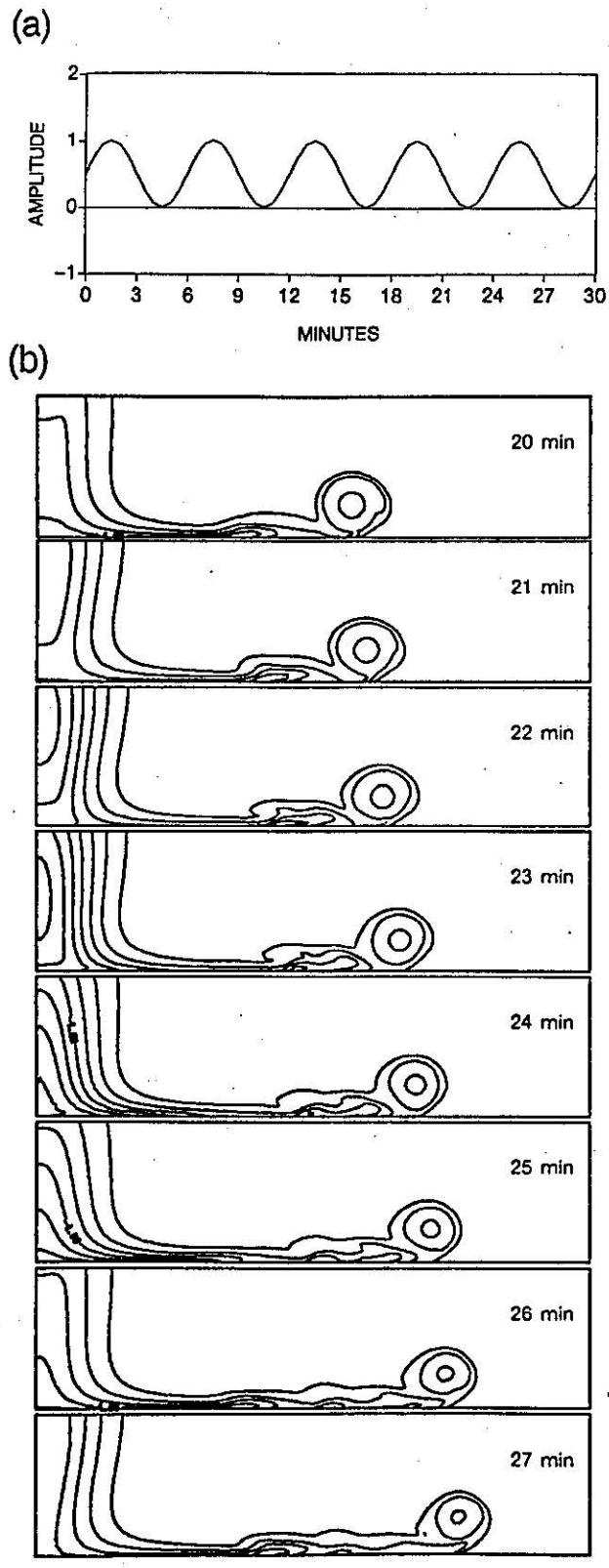

Figure 8 . **(a)** *The shape of the cooling function for pulsating flow rate experiment. Base cooling rate was −0.05 °C/s.* **(b)** *Flow resulting from pulsed forcing is shown every min from 20 to 27 min into the simulation. Potential temperature is contoured every 1°C; coldest contour is −7°C at 23 and 24 min. Domain shown is 12 km wide and 3 km high.*

three distinct subfrontal features are indeed present in the outflow, but they are spaced at roughly 2 km intervals, and the nearest of them is roughly 4 km away from the downdraft. In the DFW observations, the vortices were next to the downdraft with a spacing of at most 0.5 km. Thus it appears that Fujita's hypothesis is untenable.

Wolfson (1990) has investigated the other hypotheses put forth to explain the observed vortices in the DFW data, and found none of them to be correct. Proctor (1988) showed that his numerical model of a single microburst thunderstorm could simulate some of the features in the DFW data, but it exhibited nothing resembling the rapid oscillations in the vertical velocity and temperature thought to be due to the "vortices". What, then, did cause the wind pattern encountered by Delta 191?

5.2. A New Hypothesis

I suggest that Delta 191 actually encountered *two* thunderstorm outflows during the last 90 s of its flight. One storm was located 1 km west and 3.4 km north of runway 17L, and had a 2 km radius. The second storm was 6 min older, and was located 7.2 km north and 2.1 km east of the runway, and had a 4.75 km radius to the leading edge updraft. The embedded vortices encountered by Delta 191 were essentially an old gust front or "rotor" from this storm to the northeast. The hypothesized scenario is shown in Figure 9 .

To prove that this could indeed be the resolution of the "vortices" mystery, a numerical simulation was again performed with the help of Straka and Anderson. A neutral boundary layer axisymmetric model simulation was used for the older, distant storm (11 min simulation), and the same model with a 300 m deep stable layer, 4 K colder than the environment, was used to simulate the newer, closer storm (5 min simulation; see Figure 9). Otherwise, both models were identical with the following characteristics. The horizontal and vertical grid resolution was chosen to be 20 m. The time step was 0.1 s, the domain was 500 grid points wide by 350 high, and the eddy diffusion coefficient was 40 m^2/s. The environmental lapse rate of potential temperature was based on the profile of potential temperature measured by Delta 191. The cooling source was Gaussian in shape, with a radius of 1.0 km, and a depth of 4 km, centered at 3.5 km agl. The cooling rate was chosen so that the downdraft would be approximately 11 K colder than the neutral layer at the surface.

As can be seen in Figure 10 , the distant storm provides the oscillations in vertical velocity and temperature, and a sizable downdraft and increase in tailwind. The closer, younger storm provides the strong downdraft and tailwind, plus the crosswind blowing from west to east. The plotted dataset from Delta 191 ends at the last wind measurements, but the temperature was available for a short time afterward; it does increase just after 300 s in rough agreement with the numerical simulations.

Admittedly, not every wiggle is simulated through these two axisymmetric storm models at these times in these locations. However, a certain spatial compression and skewing of the wind features would be expected to result from the interaction of the two outflows. This comparison shows that the vortices encountered by Delta 191 were part of the actual wind pattern inside the gust front from an axisymmetric thunderstorm. In these early stages of thunderstorm out-

flow, the gust front portion of an outflow is at least as hazardous as the more laminar central downdraft.

The Stephenville radar 140 km away showed the DFW "cell" to have achieved VIP level 3 at least by 2256 GMT. By the time the accident occurred at 2305–2306, VIP level 4 was observed. I suggest both downdrafts encountered by Delta 191 came from this same radar cell; perhaps at higher resolution the individual cell components could have been identified. The same radar "cell" (different downdraft within) produced 35 m/s winds over the airport 20 min after the crash, indicating that it was indeed a multicell storm. The NSSL lightning detector observed a lightning strike about 15 min before the accident north–northeast of DFW. At this same time, observers also reported a cumulonimbus cloud north–northeast of the airport. Caracena et al. (1986) suggest that the outflow from a cell 20 km north–northeast of the airport contributed to the forcing for the DFW cell. This storm formed 20–30 min before the accident, and was visible on the Stephenville radar display. I think another, closer storm must have formed because of the observed strength of the vortices (gust front) and the cold temperature of the air. However, the evidence of older storms to the northeast clearly confirms the preferential development of new convection towards the southwest, triggered by old outflows.

Observations of the onboard weather radar of another flight airborne at the time of the crash indicated a "solid red contour (the highest contoured reflectivity) with no visible reflectivity gradients on a plan view scan. He notes having seen a green hook shaped echo (the lowest contoured reflectivity) protruding from a microburst cell over DFW airport seconds before another crew member sighted the fireball produced by Delta 191." (Caracena et al. 1986). This green thin line echo is the signature of a gust front, but it could not be the gust front from the new cell that Delta 191 encountered for two reasons. First, the gust front (leading vortex ring) would not have separated from that storm for another 2 min at least (refer to wind pattern of "new storm" in Figure 9), and second, even if the gust front had separated it would have been concentric with the cell, not "protruding". Yet this protruding gust front separated from its parent storm is exactly what would have been seen if something like the scenario in Figure 9 is correct. This provides additional support to the argument that Delta 191 encountered two outflows during its last 90 s of flight.

5.3. Other Fatal U.S. Microburst Accidents

The next most recent microburst aircraft accident was the crash of Pan American Flight 759 at New Orleans International airport on July 9, 1982. Not nearly as much information is available on this crash; unambiguous recon-

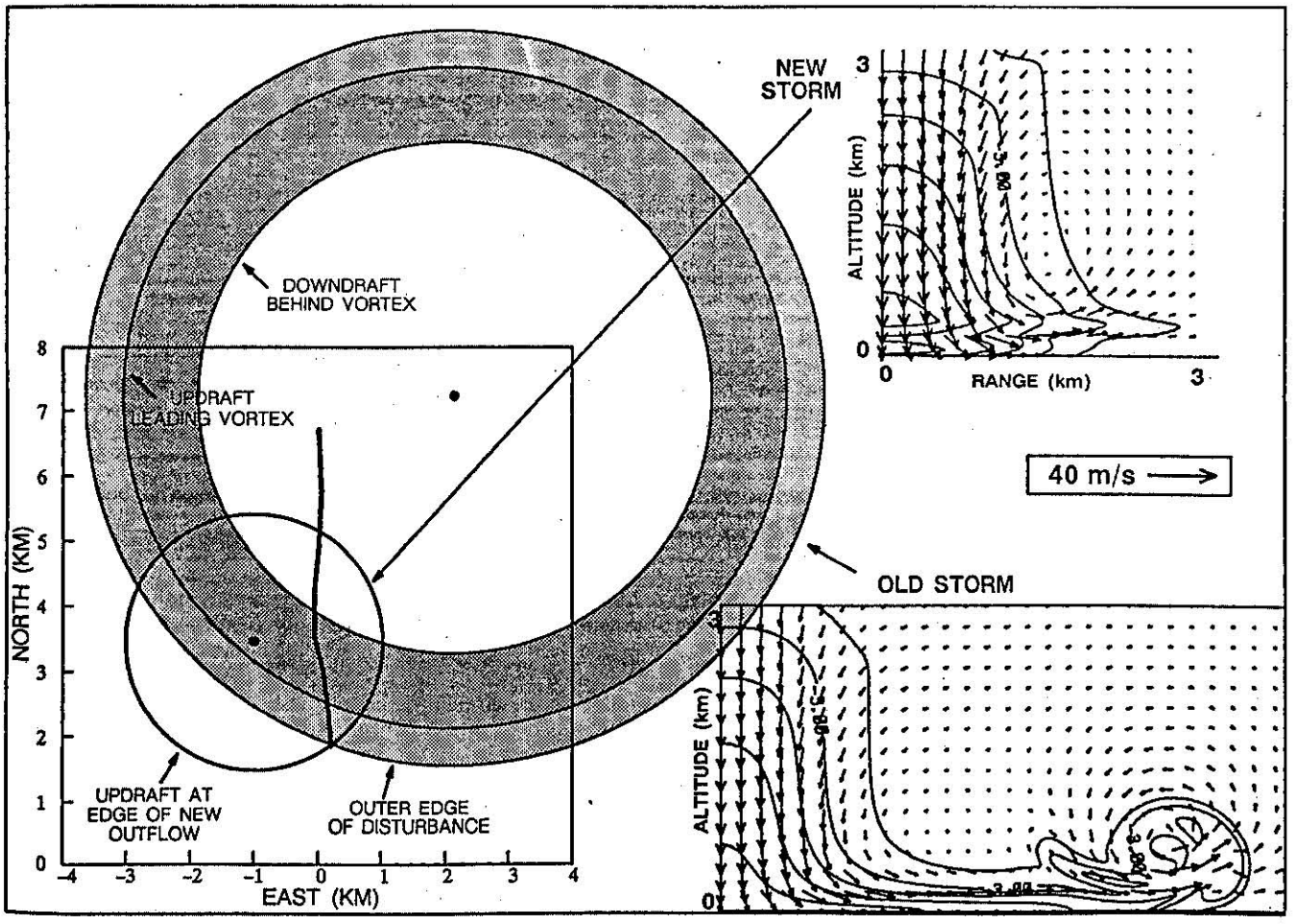

Figure 9. Proposed meteorological scenario during the crash of Delta 191 at DFW. The spots indicate thunderstorm downdraft centers. The thick black line represents the last 90 s of the Delta 191 flight. The north end of runway 17L is located at (0,0). Cross-sectional wind fields from the new and old storm are shown on the right. Potential temperature is contoured every 2°C from -1°C.

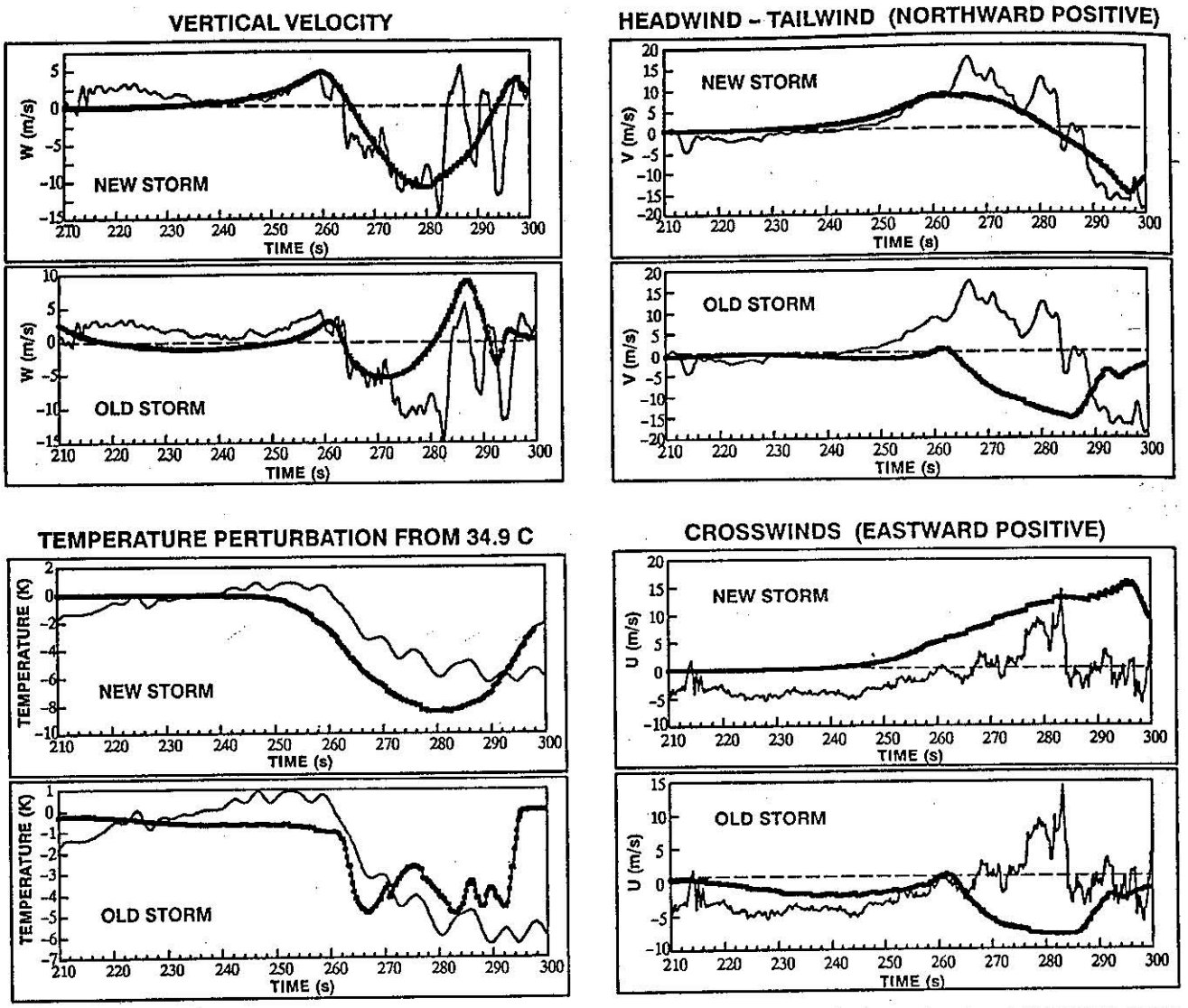

Figure 10 . Vertical velocity, north–south (headwind–tailwind) wind component, temperature perturbation, and east–west (crosswind) component from axisymmetric numerical model data (thick line), compared with Delta 191 data recovered by Wingrove and Bach (1987; thin line). For each variable, the top panel shows the model data from the closer, younger thunderstorm outflow, and the bottom panel shows the model data from the distant older outflow.

struction of the wind field was not possible. However, from Fujita's (1983) analysis, it is fairly definite that a newly formed thunderstorm downdraft and outflow occurred almost directly over the runway. It also appears that this downdraft landed just behind a gust front that had recently crossed the airport. The significance of encountering an old gust front just when the aircraft was emerging from the new downdraft is not known, but by analogy with the DFW case, this could well have contributed to the overall hazard.

Finally, we can reexamine the very first accident ever attributed to microburst wind shear, the crash of Eastern Flight 66 at JFK airport in New York on June 24, 1975. This was the accident that led to the development of the new burst terminology. Was this new downburst (later redefined as a microburst) anything other that a thunderstorm downdraft? I suggest that the presence of the sea breeze front made a fundamental difference on the evolution of the outflow pushing southward and eastward from scattered thunderstorms over the land. The winds from the sea breeze, perhaps augmented by the environmental winds, opposed the southward advancement of the thunderstorm air. Along this boundary an arc cloud developed that was visible in the satellite imagery (Fujita 1976); this indicated convergence and an updraft strong enough to raise surface air to the condensation level. As in the other two microburst accidents, the thunderstorm downdraft landed just behind a gust front. In this case, the increased flow from two preceding downdrafts, in almost the same place as the third, accident-causing downdraft, added to the circulation about the leading edge of the outflow and probably enhanced the wind shear.

5.4. Summary

The hazardous low altitude wind shear events that have caused the fatal aircraft accidents attributed to microbursts were apparently the *combination* of a precipitation driven downdraft from a thunderstorm landing within the outflow of another thunderstorm, very near or essentially on top of the leading gust front. The "fresher" that gust front, the greater the aircraft hazard. In an isolated storm, the gust front has moved far enough from the main storm

downdraft by the time it has built into a strong horizontal vortex to physically separate the two hazardous regions. The most dangerous combination appears to include a strong downdraft about 2 min after reaching the surface, landing on top of the leading vortex of a circular gust front formed no more than about 10 min previously. In this way, the turbulent hazard of the gust front is brought into the same area as the performance decreasing downdraft and divergent wind shear of the precipitation driven thunderstorm downdraft.

6. CONCLUSIONS

The primary conclusion of this work is that the fatal aircraft accidents attributed to microbursts, including the first accident for which the microburst terminology was developed, all involved the *combination* of a precipitation driven downdraft and the narrow, low altitude downdraft and turbulent region associated with a gust front.

The first part of predicting microbursts, then, is predicting the strength of the precipitation driven thunderstorm downdraft. The second, previously unrecognized part of predicting microbursts involves tracking the gust fronts from older thunderstorm outflows. These often initiate new convection, so the possibility of a new downdraft forming along a gust front is not unlikely. The presence of a relatively fresh, turbulent gust front appears to greatly increase the aviation hazard of flying through a newly formed thunderstorm outflow.

ACKNOWLEDGEMENTS

Drs. John Anderson and Jerry Straka at the University of Wisconsin were extraordinarily helpful in performing this work. All of the model simulations were performed by them with their models. Conversations with John Anderson were especially helpful. The Delta 191 wind and temperature data were graciously supplied by Rodney Wingrove at NASA Ames.

REFERENCES

Addis, R.P., 1984: A numerical model of surface outflows from convective storms. *Boundary-Layer Meteor.*, 28, 121–160.

Anderson, J.R., 1990: Numerical simulation of thunderstorm microburst outflows. Submitted to *Mon. Wea. Rev.*

Biron, P.J., and M.A. Isaminger, 1989: An analysis of microburst characteristics related to automatic detection from Huntsville, AL and Denver, CO. Preprints, *24th Conference on Radar Meteorology*, Tallahassee, Amer. Meteor. Soc., 269–273.

Burrows, D.A., and L.F. Osborne, 1986: Precipitation loading in wet microbursts. Preprints, *23rd Conference on Radar Meteorology*, Snowmass, Amer. Meteor. Soc., J97–J100.

Caracena, F., R. Ortiz, J. Augustine, 1986: The crash of Delta Flight 191 at Dallas-Fort Worth International Airport on 2 August 1985: Multiscale analysis of weather conditions. *NOAA Tech. Rep. ERL 430-ESG 2*, 33pp.

Droegemeier, K.K. and M.R. Babcock, 1989: Numerical simulation of microburst downdrafts: Application to on-board and look-ahead sensor technology. *AIAA 27th Aerospace Sciences Meeting*, AIAA-89-0821, Reno, 12 pp.

Evans, J., and D. Turnbull, 1989: Development of an automated windshear detection system using Doppler weather radar. *Proc. IEEE*, 77, 1661–1673.

Fawbush, E.J., and R. C. Miller, 1954: A basis for forecasting peak wind gusts in non-frontal thunderstorms. *Bull. Amer. Meteor. Soc.*, 35, 14–19.

Frost, W., and R.L. Bowles, 1984: Wind shear terms in the equations of aircraft motion. *J. Aircraft*, 21, 866–872.

Fujita, T.T., 1976: Spearhead echo and downburst near the approach end of a John F. Kennedy airport runway, New York City. *SMRP Res. Pap. 137*, University of Chicago, Ill., 51 pp.

Fujita, T.T., 1983: Microburst wind shear at New Orleans International Airport, Kenner, Louisiana on July 9, 1982. *SMRP Res. Pap. 199*, University of Chicago, Ill., 39 pp.

Fujita, T.T., 1984: Andrews AFB microburst: Six minutes after the touchdown of Air Force One. *SMRP Res. Pap. 205*, University of Chicago, Ill., 38 pp.

Fujita, T.T., 1985: *The Downburst – Microburst and Macroburst*. Satellite and Mesometeorology Project, Department of the Geophysical Sciences, The University of Chicago, Ill., 122 pp.

Fujita, T.T., 1986: *DFW Microburst*. Satellite and Mesometeorology Project, Department of the Geophysical Sciences, The University of Chicago, Ill., 154 pp.

Fujita, T.T., and H. R. Byers, 1977: Spearhead echo and downburst in the crash of an airliner. *Mon. Wea. Rev.*, 105, 129–146.

Garvine, R.W., 1984: Radial spreading of buoyant, surface plumes in coastal waters. *J. Geophys. Res.*, 89, No. C2, 1989–1996.

Goff, R.C., 1976: Vertical structure of thunderstorm outflows. *Mon. Wea. Rev.*, 104, 1429–1440.

Kingsmill, D.E., R.M. Wakimoto, and W.C. Lee, 1989: Kinematic and dynamic analysis of microburst producing thunderstorm. Preprints, *24th Conference on Radar Meteorology*, Tallahassee, Amer. Meteor. Soc., 146–149.

Knupp, K.R., 1987: Downdrafts within High Plains cumulonimbi. Part I. General kinematic structure. *J. Atmos. Sci.*, 44, 987–1008.

Krueger, S.K., and R.M. Wakimoto, 1985: Numerical simulation of dry microbursts. Preprints, *14th Conference on Severe Local Storms*, Indianapolis, Amer. Meteor. Soc., 163–166.

Laynor, W.G., 1986: Summary of windshear accidents and views about prevention. *Wind Shear – SAE SP-681*, No. 861697, 1–12.

Linden, P.F., and J.E. Simpson, 1986: Gravity-driven flows in a turbulent fluid. *J. Fluid Mech.*, 172, 481–497.

Proctor, F.H., 1989: Numerical simulations of an isolated microburst. Part II: Sensitivity experiments. *J. Atmos. Sci.*, 46, 2143–2165.

Rudich, R.D., 1986: Weather-involved U.S. air carrier accidents 1962–1984: A compendium and brief summary. *AIAA 24th Aerospace Sciences Meeting*, AIAA-86-0327, Reno, 7 pp.

Simpson, J.E., 1987: *Gravity Currents in the Environment and the Laboratory*. Ellis Horwood Ltd., 244 pp.

Smith, R.K., 1988: Travelling waves and bores in the lower atmosphere: The "Morning Glory" and related phenomena. *Earth-Sci. Rev.*, 25, 267–290.

Srivastava, R.C., 1985: A simple model of evaporatively driven downdraft: Application to a microburst downdraft. *J. Atmos. Sci.*, 42, 1004–1023.

Targ, R., and R.L. Bowles, 1988: Windshear avoidance: Requirements and proposed system for airborne lidar detection. *Airborne and Spaceborne Lasers for Terrestrial Geophysical Sensing, SPIE Vol. 889*, 54–64.

Wakimoto, R.M., and V.N. Bringi, 1988: Dual polarization observations of microbursts associated with intense convection: The 20 July storm during the MIST project. *Mon. Wea. Rev.*, 116, 1521–1539.

Wakimoto, R.M., C.J. Kessinger, and D.E. Kingsmill, 1989: Visual and dual-Doppler analysis of low-reflectivity microbursts. Preprints, *24th Conference on Radar Meteorology*, Tallahassee, Amer. Meteor. Soc., 77–80.

Wilson, J.W., R.D. Roberts, C. Kessinger, and J. McCarthy, 1984: Microburst wind structure and evaluation of Doppler radar for airport wind shear detection. *J. Climate Appl. Meteor.*, 23, 898–915.

Wingrove, R.C., and R.E. Bach, 1987: Severe winds in the DFW microburst measured from two aircraft. *AIAA Guidance, Navigation, and Control Conference*, AIAA-87-2340,477-482.

Wolfson, M.M., 1990: *Understanding and Predicting Microbursts*. Ph.D. thesis, Massachusetts Institute of Technology, 303 pp.

Zorpette, G., 1986: The menacing microburst. *IEEE Spectrum*, 23, 50–56.